BMC Public Health

Human behaviour, NPI and mobility reduction effects on COVID-19 transmission in different countries of the world

Zahra Mohammadi[1*†], Monica Gabriela Cojocaru[1†] and Edward Wolfgang Thommes[1,2†]

Abstract

Background: The outbreak of Coronavirus disease, which originated in Wuhan, China in 2019, has affected the lives of billions of people globally. Throughout 2020, the reproduction number of COVID-19 was widely used by decision-makers to explain their strategies to control the pandemic.

Methods: In this work, we deduce and analyze both initial and effective reproduction numbers for 12 diverse world regions between February and December of 2020. We consider mobility reductions, mask wearing and compliance with masks, mask efficacy values alongside other non-pharmaceutical interventions (NPIs) in each region to get further insights in how each of the above factored into each region's SARS-COV-2 transmission dynamic.

Results: We quantify in each region the following reductions in the observed effective reproduction numbers of the pandemic: i) reduction due to decrease in mobility (as captured in Google mobility reports); ii) reduction due to mask wearing and mask compliance; iii) reduction due to other NPI's, over and above the ones identified in i) and ii).

Conclusion: In most cases mobility reduction coming from nationwide lockdown measures has helped stave off the initial wave in countries who took these types of measures. Beyond the first waves, mask mandates and compliance, together with social-distancing measures (which we refer to as *other NPI's*) have allowed some control of subsequent disease spread. The methodology we propose here is novel and can be applied to other respiratory diseases such as influenza or RSV.

Keywords: SEIRL model, Initial and effective reproduction number, Mobility, Mask: adoption, Compliance & efficacy, Pandemic control

Background

The first known case of disease caused by SARS-CoV-2 was identified in Wuhan, China, in December 2019. The disease spread worldwide in a few weeks, leading to a pandemic still ongoing as of the winter of 2022.

Since December 2019, the basic and effective reproduction number of COVID-19 have been continuously discussed by scientists, political decision-makers and the media (regular and social). The basic reproduction number of an infectious disease, denoted by R_0, represents the expected number of new cases generated by a single infectious individual in a fully susceptible population. In epidemiology, a pandemic will be under control and the transmission will die out when $R_0 < 1$. The basic reproduction number of infectious disease

†Zahra Mohammadi, Monica Gabriela Cojocaru and Edward Wolfgang Thommes contributed equally to this work.

*Correspondence: zahram@uoguelph.ca

[1] Department of Mathematics & Statistics, University of Guelph, 50 Stone Road E., Guelph N1G 2W1, Canada
Full list of author information is available at the end of the article

Mohammadi *et al. BMC Public Health*   (2022) 22:1594

Page 2 of 19

depends on the behavioural activity in local populations (behavioural activity between infector-infectee). The basic reproduction number for COVID-19 was reported to take values from 2.2 [1] to 6.33 [2] in different countries. In general, although whole populations started with being susceptible to virus, the progression of the pandemic steadily decreased the number of susceptibles in each region. Consequently, the average number of secondary cases per infectious case changed as the population became immunized (by recovering or dying). Thus as the pandemic progressed, R_0 gives way to the effective reproductive number, denoted by R_{eff}, which measures the average number of secondary cases per infectious case in a population at any specific time (where only a fraction is susceptible) [3]. In epidemiology, R_{eff} is a monitoring indicator of progress in controlling a pandemic. It can also be a way to monitor the effectiveness of interventions (both the effect of immunity and of additional non-pharmaceutical interventions) during a pandemic.

Transmission of SARS-COV-2 depends on the rate of person-to-person contact and on the probability of transmission given one meaningful contact between an infected and a susceptible individual. Non-pharmaceutical interventions (NPI's) are widely used in many countries in 2020 to reduce the rate of person-to-person contact and the probability of transmission per contact in the absence of vaccine. The wearing of masks [4, 5] and the effectiveness of mask-wearing in preventing transmission of SARS-CoV-2 was not recognized in some world regions during the first several months of the pandemic, despite the effectiveness of public mask use in controlling the spread of the 2003 SARS [6, 7].

Another critical non-pharmaceutical intervention for slowing epidemic growth is social distancing which includes shelter-in-place requirements, prohibition of indoor gatherings, imposition of travel restrictions, school closures and workplace closures. Previous studies investigated the quantitative relationships between the COVID-19 epidemic parameters (for instance the total death toll) and social distancing efforts [8–11]. Mobile data provide a unique opportunity to investigate to some degree the effectiveness of social distancing measures in reducing the effective reproduction number of COVID-19 [12–14]. Mobile data can be interpreted as a proxy of person-to-person contact reduction as a consequence of social distancing measures, although it generally does not capture short-range behavioral changes, such as maintaining a 6 foot spacing between individuals in public settings. The publicly available data on human mobility that is

provided by Google, Apple, Facebook, etc have been used in several articles to evaluate the effectiveness of non-pharmaceutical interventions (NPIs) on the spread of COVID-19 [15–20].

Existing pre-pandemic work, such as [21–23], represents the effect of the population-level contact patterns on the infection transmission dynamics. The infection transmission rate varies in different countries as a result of the different social and economic structures and different contact patterns. Mistry et al. [22] used the derived contact matrices to model the spread of airborne infectious diseases. The transmission rate of COVID-19 fundamentally depends on interpersonal interaction rates. Most countries considered different strategies for reducing the contact rate in order to control the spread of the virus. Feehan and Mahmud calculated age-structured contact matrices to quantify how much interpersonal contact has changed during the pandemic in the United States [24]. They estimated about 82% decline in interpersonal contact between March 22nd and April 8-th, 2020 (known as wave 0) and an increase in daily average contact rates over the subsequent waves. Other studies observed the decline in contact rates in China [25], United Kingdom [26], Luxembourg [27], Italy, Belgium, France, and the Netherlands [28] throughout the pandemic. Prem et al. created synthetic contact matrices to represent the effect of intervention measures to reduce social mixing on outcomes of the COVID-19 epidemic in Wuhan, China [29, 30]. The age-specific social contact characterization also supports the possibility of suspecting differences in transmission patterns of COVID-19 outbreak among different age-groups [20, 31–33]. In this work, projected contact matrices provided by Prem et al. [21] are used.

This work presents a SEIRL (Susceptible, Exposed, Infectious, Recovered and isoLated) model that uses incidence data, Google mobility data (as a modifier of effective contact rates), mask efficacy assumption and mask compliance data to provide insight into the strategies employed for controlling the pandemic in each country/region under consideration. It explores and quantifies the effectiveness of non-pharmaceutical policy interventions across 10 diverse countries and one province in Canada and one state in the united states, using their effective reproduction number R_{eff}. To accomplish these goals we estimate the R_0 values of each region (using the classic next-generation matrix analysis [34]) and then a time-dependent effective reproduction number, denoted by $R_{eff-data}$, using known repositories of incidence data for each country [35]. Using the projected contact rates from [21]

Mohammadi *et al. BMC Public Health*   (2022) 22:1594

Page 3 of 19

Table 1 Countries under consideration

	Regions	Population Density	GDP	Median Age	Urbanization
1	Ontario	37.9/sq mi	710	40.4	86.2
2	Florida	384.3/sq mi	1095.9	42.5	91.2
3	Romania	218.6/sq mi	248.6	42.5	56.4
4	Sweden	64.7/sq mi	529.1	41.1	88
5	Italy	521.4/sq mi	1848.2	46.5	71
6	Ghana	262.9/sq mi	67.3	21.4	57.3
7	South Africa	109.8/sq mi	282.6	28	67.4
8	Saudi Arabia	38.8/sq mi	680.9	30.8	84.3
9	Indonesia	357.4/sq mi	1089	31.1	56.6
10	Nepal	466.2/sq mi	32.2	25.3	20.6
11	Brazil	64.7/sq mi	1363.8	33.2	87.1
12	Argentina	37.3/sq mi	382.8	32.4	92.1

extrapolated to each country of interest with publicly available demographic data, we also infer the time-dependent effective contact rates, and hence the time-dependent effective reproduction number of each country as a function of multiple Google mobility indices. We denote this by $R_{eff-mobile}$. We compute the time-dependent effective reproduction influenced by mobility reduction, mask efficacy and mask compliance data that is denoted by $R_{eff-mobilemask}$ here.

Comparing the two estimates of R_{eff} we investigate the effect of NPI's, over and above changes in contact rates due to mobility and mask mandates, in each country's epidemiology throughout the year 2020[1]. It is concluded in most cases that mobility reduction coming from stringent lockdown measures helped stave off the initial wave in countries which took these types of measures (see for instance Fig. 2). While mobility increased in the second part of 2020 (see Fig. 7), mask mandates together with all other NPI measures (for instance social-distancing) have allowed some "control" of subsequent waves, in the sense that countries were able to maintain their effective reproduction numbers around 1.

The structure of the paper is as follows: Section Methods and model setup presents the setup and methodology employed in the analyses of each of the twelve regions. Section Results and discussion presents the results and discussion on quantification of the reduction in the effective reproduction numbers $R_{eff-mobile}$ and $R_{eff-mobilemask}$, as well as the estimated effective reproduction numbers based on incidence

data $R_{eff-data}$. The paper closes with a discussion of the results and a few directions for future work.

Methods and model setup

We chose 10 countries around the world, one U.S. state (Florida) and one province of Canada (Ontario), based on a diversity of characteristics: population density, median age, urbanization of population and gross domestic product (GDP) in 2020 (theses various characteristics are presented in Table 1 below:

The data are collected from IndexMundi. In each of these regions we are interested to model the pandemic evolution during the year 2020 via a SEIRL model described below.

Susceptible individuals (denoted by S and considered to be the entire population initially) exposed to the virus enter the exposed (E) compartment for an average of $1/\sigma$ days before they become contagious, at which point they move into the I (infected) compartment. In general, there is an a proportion of infected individuals who will not develop symptoms (so-called asymptomatic, denoted by I^A), while the remaining $1-a$ percentage make up the infected symptomatic individuals, denoted by I^S. Thus here:

$$I(t) = I^A(t) + I^S(t) = aI(t) + (1-a)I(t). \qquad (1)$$

An ε proportion of $I^S(t)$ will self-isolate into the L (isolated) compartment. They do so with a delay of $1/\kappa$ days, accounting for a test result wait time and/or individuals who may disregard minor symptoms initially. After $1/\gamma$ days, individuals recover from (or succumb to) their infection and move into the R (recovered) compartment.

A diagram of the process we model is as follows (Fig. 1):

---

[1] We chose to concentrate on the year 2020 specifically because there were no preventative or antiviral treatments known against this virus at that time, and countries had to rely on some combination of NPI's to fight its spread.

Mohammadi *et al. BMC Public Health* (2022) 22:1594

Page 4 of 19
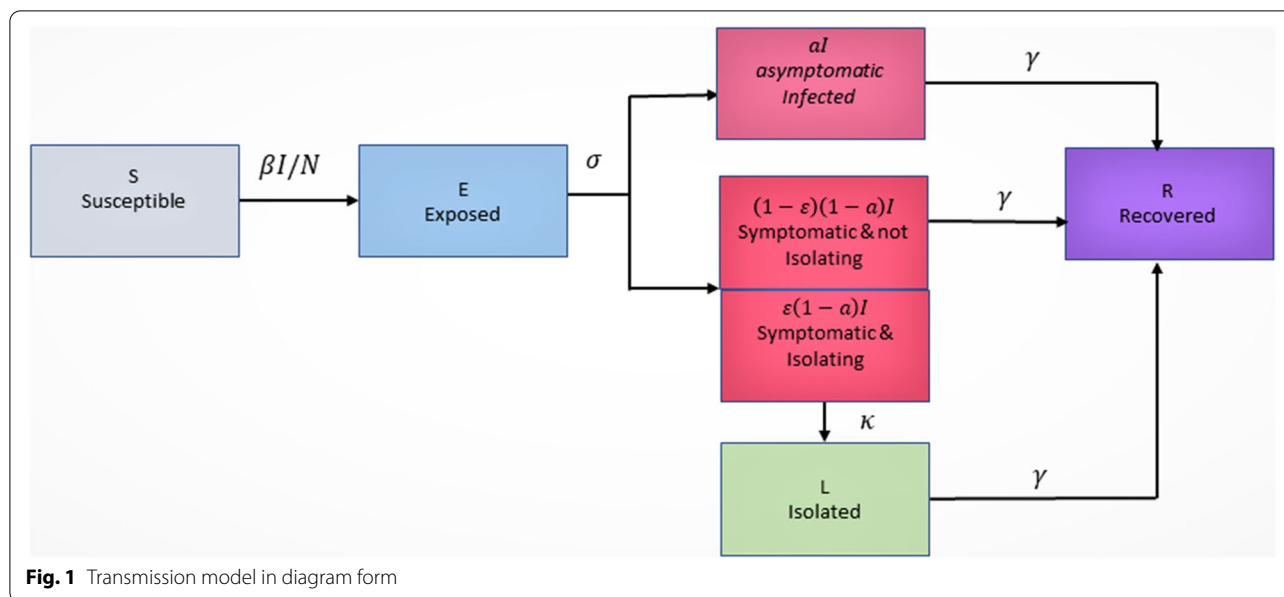
Fig. 1 Transmission model in diagram form

Using the expressions in (1) and model Fig. 1, we obtain the following equations:

$$
\begin{cases}
\dfrac{dS}{dt} = -\beta S(t)\dfrac{I(t)}{N_{total}}, \\[2mm]
\dfrac{dE}{dt} = \beta S(t)\dfrac{I(t)}{N_{total}} - \sigma E(t), \\[2mm]
\dfrac{dI}{dt} = \sigma E(t) - \gamma I(t) + \epsilon(\gamma - \kappa)(1-a)I(t) \\[2mm]
\dfrac{dL}{dt} = \epsilon\kappa(1-a)I(t) - \gamma L(t). \\[2mm]
\dfrac{dR}{dt} = \gamma(1 - \epsilon(1-a))I(t) + \gamma L(t).
\end{cases}
\tag{2}
$$

Our model parameters have been taken from literature (as can be seen in Table 2), with the exception of the proportion of infected who isolate, ε, which we assume to be equal to 95%, and the isolation rate κ.

in our papers [41, 42], where the compartmental models were slightly different.

We obtain its closed form expression:

$$
R_0 = \frac{\beta(t=0)}{(\epsilon\gamma a - \epsilon\kappa a - \epsilon\gamma + \epsilon\kappa + \gamma)}.
\tag{3}
$$

where $\beta(t=0)$ is the initial value of β. As β subsequently changes over time with evolving control measures, we transition from the basic reproduction number to a time-dependent "control reproduction number" (see [43, 44]),

$$
R_c = \frac{\beta(t)}{(\epsilon\gamma a - \epsilon\kappa a - \epsilon\gamma + \epsilon\kappa + \gamma)}.
\tag{4}
$$

We can also estimate R_0 as a function of the growth factor near the DFE in each region using (3) (see more details in Additional file 1: Appendix):

$$
R_c(\rho) = \frac{\epsilon\gamma a\rho + \epsilon\gamma a\sigma - \epsilon\kappa a\rho - \epsilon\kappa a\sigma - \epsilon\gamma\rho - \epsilon\gamma\sigma + \epsilon\kappa\rho + \epsilon\kappa\sigma + \gamma\rho + \gamma\sigma + \rho^2 + \rho\sigma}{\sigma(\epsilon\gamma a - \epsilon\kappa a - \epsilon\gamma + \epsilon\kappa + \gamma)}
\tag{5}
$$

Time series of effective reproduction numbers using a near-disease-free equilibrium estimate and incidence data

The Jacobian analysis near the disease-free equilibrium (DFE) which consists of $S(0)=N$ and $I(0)=0$ for the system (2) and the next generation matrix method [34] for computing the initial R_0 are given in Additional file 1: Appendix. We have employed a similar type of approach

To estimate the exponential growth factor for each region as a time series, we rely on weekly case incidence data (which we denote by $inc(t)$) for each region. We assume that $inc(t)$ is given by an exponential curve of the type:

$$
inc(t) = inc(0)e^{\rho t}.
$$

In this case, we can compute a time-series of the exponential growth factor:

Table 2 Parameter values for our model 2

Symbol	Definition	Initial Value	Reference
N_{total}	Population size	Table 4	
σ	Rate at which exposed become infectious (days $^{-1}$)	1/2.5	[36]
a	Proportion of permanently asymptomatic cases	0.5	[37],[38],[39]
ε	Proportion of compliance with isolation	0.95	assumed
κ	Isolation rate	1	assumed
γ	Recovery/removal rate	1/7	[40]

$$\rho(t) = \ln \frac{inc(t+1)}{inc(t)}, \text{ with } inc(t) \neq 0.$$

Using this time series of $\rho(t)$ in Eq. (5) we obtain a time series for the effective reproduction number:

$$R_{eff-data}(t) = R_c(\rho(t))s(t), \text{ where } s(t) \text{ represents the remaining fraction of susceptibles at each } t, \qquad (6)$$

i.e. the difference between the entire population and the current cumulative number of infected individuals:

$$s(t) = 1 - \frac{1}{N}\left(\sum_{\tau \in [0,t]} inc(\tau)\right)$$

Figure 2 represents the weekly changes in the effective reproduction numbers of incidence data, $R_{eff-data}$ that is explained in section (Time series of effective reproduction numbers using a near-disease-free equilibrium estimate and incidence data), throughout 2020 for each geographical location under study. The vertical lines in each panel represent the dates in which local governments have introduced nationwide measures: in most countries lockdown measures took effect, while in Sweden and Indonesia partial lockdown measures were in place. In Sweden, nationwide lockdown was considered to be a violation of people's freedom of movement. The government strategy was based on individual responsibility. Measures included were: border closures, recommendations about social distancing, and traveling. Local reports show a 50% drop in public transport usage in April for the Swedish counties [45],[46]. In Stockholm, a 30% drop in the number of cars [47], and 70% fewer pedestrians [48] was reported in April 2020. Later in November, the Swedish government imposed mandatory restrictions as well (e.g. all gatherings of more than eight people were banned).Italy had one of the earliest implementations of lockdown, as early as February 23, 2020. We showcase all dates for all locations in Table 3.

Data sources
In the remainder of the paper we use various sources of publicly-available data. First we use Google data mobility [49] for each region of interest. Then we use Johns Hopkins data for case incidence: incidence [35] and we use the Prem et al. [21] paper and their contact data projections (where projections for provinces or states in Canada and the US were obtained by using the projections weighted with population data for such provinces or states. Lockdown measures start dates have been taken from the ascent of the Oxford stringency index at Financial Times.

Population data were obtained from Stats Canada [50], US Census data [51], whereas for other countries we used the online repository: World age distribution [52]. For obtaining data on mask wearing compliance we used Mask Compliance [53] and European-countries [54].

Time-series of effective reproduction numbers accounting for mobility data and projected contact rates
We first devise a mechanism to mix the daily average contact rates in each region's population with the behavioural activity in that population. In Prem et. al. [21] the authors compute projected daily average contact rates for 157 countries. Specifically, they estimate the average contacts for categories of activities during a typical day, such as: home, work and other locations. They present their results for a population stratified by age, and divided into 16 age subgroups. We amalgamated the average contact rate in home, work, and other locations, then we computed the weighted average of a given projected contact matrix in a region with the corresponding proportions of 5-year age population groups in 2020 to determine one single average contact rate. We consider this last value as the average baseline (pre-lockdown) contact rate in that region (for instance, for Ontario it was computed to be: *contact$_{av}$*≈11.04). All regions' average contacts are reported below in Table 4.

Google reports contain changes in movement over time, compared to baseline (pre-lockdown) activity

Mohammadi *et al. BMC Public Health*   (2022) 22:1594

Page 6 of 19
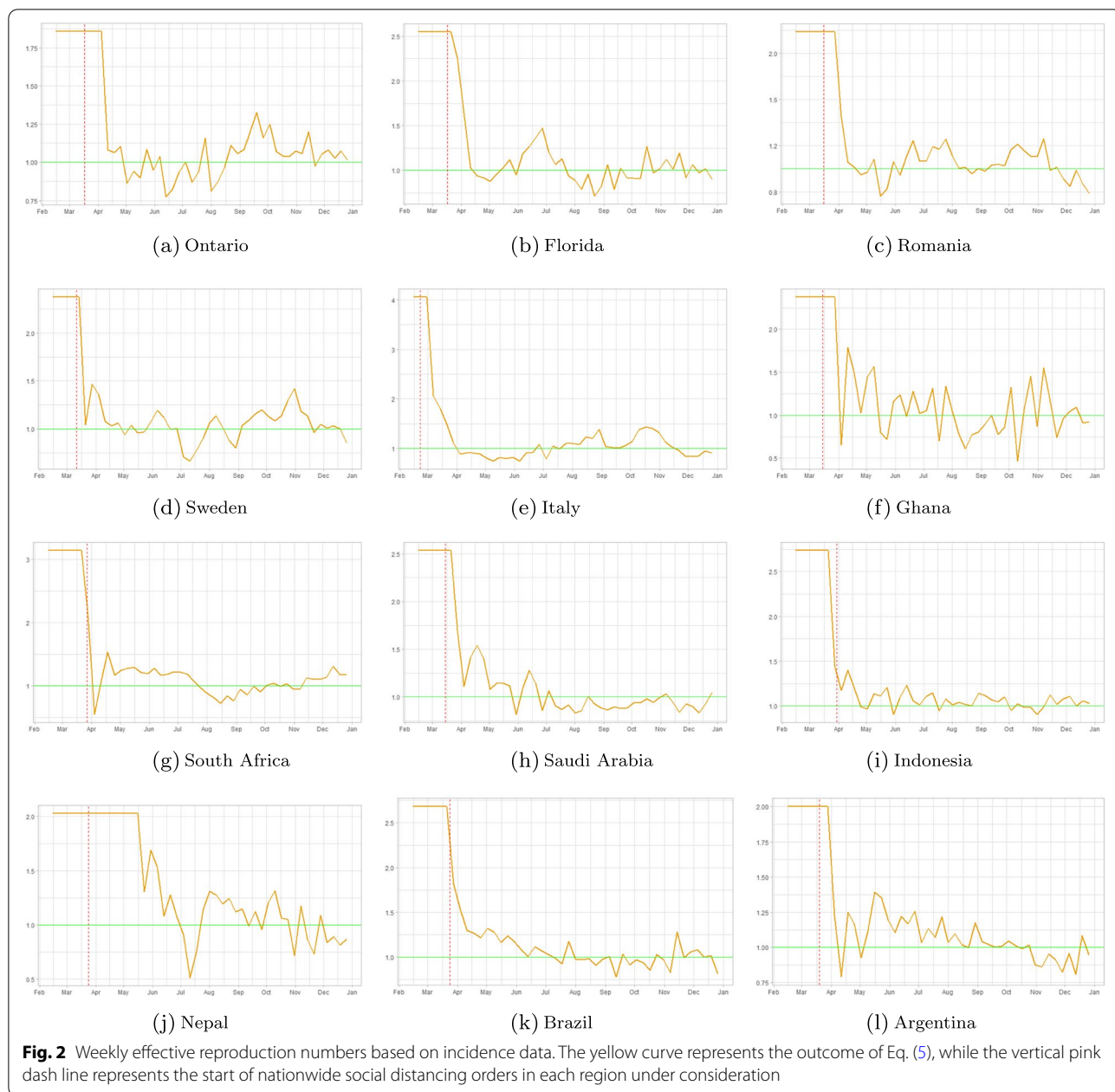
Fig. 2 Weekly effective reproduction numbers based on incidence data. The yellow curve represents the outcome of Eq. (5), while the vertical pink dash line represents the start of nationwide social distancing orders in each region under consideration

in six categories: retail/recreation, groceries/pharmacies, parks, transit stations, workplaces, and domiciles (COVID-19 Community Mobility Reports) [49]. We have used the Google index data in other works, see [20, 55].

rate for the home, work, and other location categories (comprising retail/recreation and groceries/pharmacies) from Prem et al. [21] for each region. Next, we used these category rates to modify the same categories of mobility data as follows:

$$contact_{av}^m(t) = contact_{av}^m \cdot g^m(t) \text{ where } m \in \{\text{Home, Work, Other location}\}, \ t = 1, 2, \dots \text{ week}$$

To find the mobility-influenced, time-dependent contact rates post-lockdown, we considered the average contacts

and where $g^m(t)$ is the percentage increase or decrease in the category m of mobility as compared to Google's baseline values per category. Finally, we amalgamated the

Mohammadi *et al. BMC Public Health*   (2022) 22:1594

Page 7 of 19

Table 3 Nonpharmaceutical Interventions (NPIs) measures in 2020

	Regions	Hard/partial Lockdown order	Mask Mandate
1	Ontario	17 March	17 July
2	Florida	17 March	25 June
3	Romania	16 March	1 August
4	Sweden *	11 March	7 December
5	Italy	22 February	7 October
6	Ghana	15 March	15 June
7	South Africa	27 March	1 May
8	Saudi Arabia	15 March	22 May
9	Indonesia	30 March	5 April
10	Nepal	24 March	31 July
11	Brazil	24 March	2 July
12	Argentina	19 March	29 August

Google mobility-influenced contact rates of these categories to compute the weekly mobility-influenced contact rate:

$$contact_{av}(t) = \sum_m contact_{av}^m(t) \text{ where } m \in \{\text{Home, Work, Other location}\}$$

Let us now refine our view of the effective reproduction number $R_{eff}=R_0 s(t)$ from the perspective of the changes in contact rates due to mobility reduction. From the last section we know that $R_0 = \frac{\beta}{(\epsilon\gamma a - \epsilon\kappa a - \epsilon\gamma + \epsilon\kappa + \gamma)}$, however now we have

$$\beta(t) = contact_{av}(t) \cdot p \implies R_{eff-mobile} = \frac{contact_{av}(t) \cdot p}{(\epsilon\gamma a - \epsilon\kappa a - \epsilon\gamma + \epsilon\kappa + \gamma)}(1 - \sum_{\tau \in [0,t]} inc(\tau)), \quad (7)$$

where p is the probability of transmission per meaningful contact. To estimate p, we need to have a handle on the values of R_0 from incidence data as well. To estimate R_0 from incidence data we used Eq. (5). The growth factor ρ is computed from the initial phase of (close to) exponential growth in the neighbourhood of the DFE, which corresponds to a phase of linear growth in *log(inc)*, with slope ρ. We identify the initial, fastest phase of nearly unchecked growth in any given region with the help of a piecewise linear fit to the log of the incidence. We utilize the R function dpseg(), which is a part of the dpseg package, https://cran.r-project.org/web/packages/dpseg/index.html. This function uses a dynamic programming algorithm to generate an optimal piecewise linear fit to a time series, which balances goodness of fit against an (adjustable) penalty for each additional segment. We then identify the earliest segment with the steepest positive slope (largest ρ) as corresponding to the initial near-unchecked exponential growth phase. We report the values we obtain in Table 4[2].

Table 4 summarizes the basic reproduction number R_0 at the beginning of the COVID-19 outbreak and the average contact rate (before pandemic). The basic reproduction number R_0 has maximum values in Italy and South Africa with 4.05 and 3.14, and minimum values in Ontario and Argentina with 1.85 and 1.99. We use the mask compliance data for each region (see Table 1 in Additional file 1: Appendix).

Results and discussion

Quantifying the effective reproduction number using incidence data

To quantify the overall relative status of the pandemic at the various locations, we show in Fig. 3 the evolution of $R_{eff-data}$ in each region using a heatmap plot and depicting values of $R_{eff-data}(t) \in [0,4]$.

The color gradient signifies lowest values of the effective reproduction numbers in lightest color zones, and highest values in darkest zones. Figure 3 showcases a comparison of the $R_{eff-data}$ between locations.

We can immediately see the effect of the reduction in $R_{eff-data}$, across the board, in all countries between March and April, and the rest of the year. It is clear that the initial lockdowns and mobility reduction allowed all countries to drop their $R_{eff-data}$ to around 1, and interestingly most remained around this value for the rest of 2020. We include here (Table 5) the approximate weekly average value of $R_{eff-data}$ at each location in mid-to -end of April 2020..

Qualitatively, we can understand why $R_{eff-data}$ has generally fluctuated in the vicinity of 1: On the one hand, rapid growth of incidence causes alarm at both the policymaker and individual level, and typically leads to increased NPI directives as well as compliance. On the other hand, because these measures are hard to maintain and economically taxing, NPIs are generally relaxed not long after incidence starts to drop. In other

---

[2] The last column in Table 4 highlights the number of weeks that dpseg is assigning for the steepest slope. The weeks are numbered from the first week with positive cases in each location, so near disease-free.

Mohammadi *et al. BMC Public Health* (2022) 22:1594

Page 8 of 19

Table 4 The basic reproduction number, R_0, at the beginning of the COVID-19 pandemic and contact average rate, $contact_{av}$, before the COVID-19 outbreak for each geographical location under study. The table also contains total population numbers, the growth factor in the neighbourhood of the DFE (ρ), and duration of initial exponential growth phase

	Region	Population N_{total}	$contact_{av}$	R_0	ρ	Duration of initial exponential growth phase weeks
1	Ontario	14,734,014	11.04531438	1.856251	1.239646	5
2	Florida	21,477,737	10.50481103	2.547635	2.044037	2
3	Romania	19,237,682	10.53032815	2.183026	1.63537	3
4	Sweden	10,099,270	11.09614737	2.372179	1.851232	4
5	Italy	60,461,828	12.38928992	4.054303	3.485834	2
6	Ghana	31,072,945	16.04056691	2.373496	1.852704	2
7	South Africa	59,308,690	13.21954859	3.143281	2.654134	2
8	Saudi Arabia	34,813,867	13.26255761	2.533263	2.028494	2
9	Indonesia	273,523,621	12.54859287	2.733693	2.241501	2
10	Nepal	29,136,808	16.09865556	2.025042	1.447956	2
11	Brazil	212,559,409	12.72484009	2.680081	2.185299	2
12	Argentina	45,195,777	12.13054343	1.998173	1.415379	3
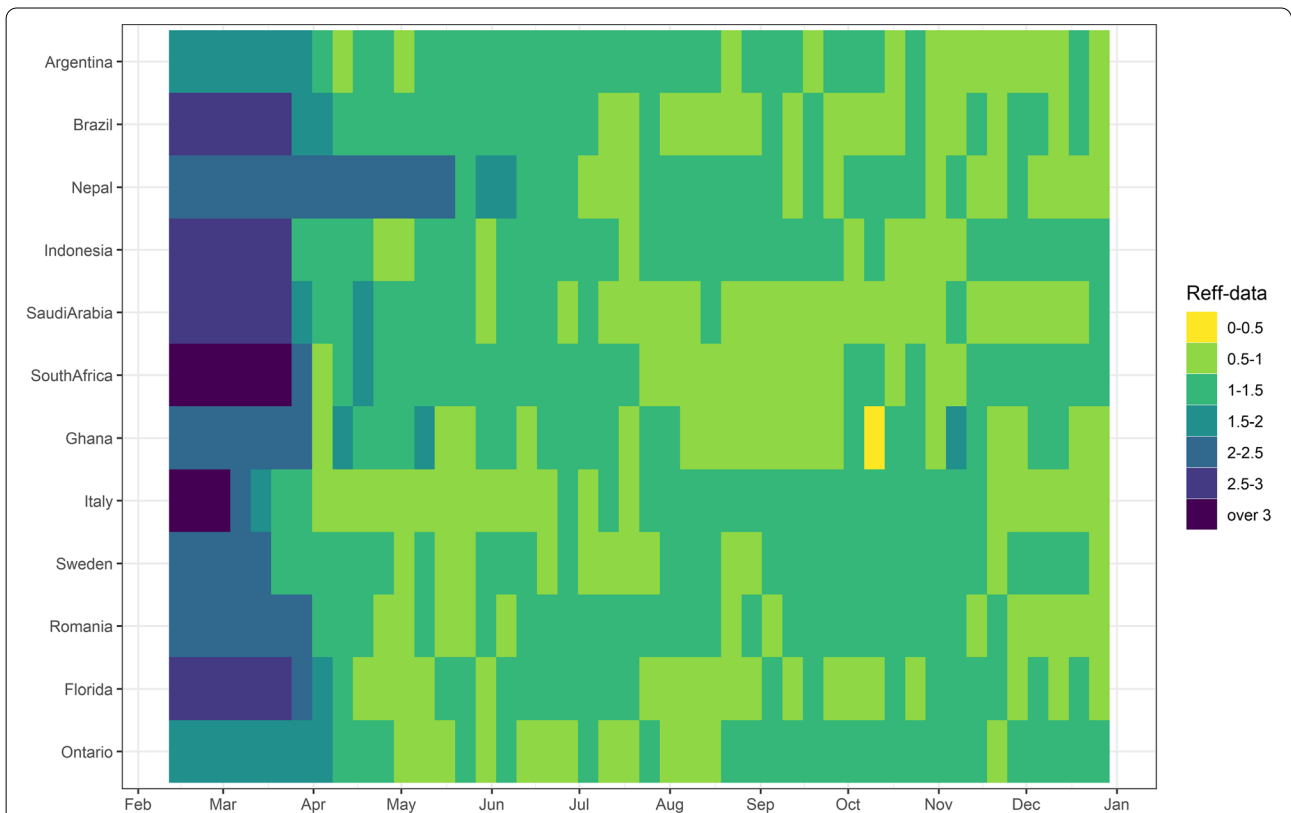
Fig. 3 The effective reproduction numbers from incidence data plotted per range of values ($R_{eff-data} \in \{[0,0.5],[0.5-1],...,[2.5-3]\}$) from February 15 to December 31, 2020. Lightest color patches signify biggest weekly reductions in values of $R_{eff-data}$ among other weeks in each region

Table 5 Average $R_{eff-data}$ at each location after the initial drop

Ontario	Florida	Sweden	Italy	Romania	Saudi Arabia	Indonesia	Nepal	South Africa	Brazil	Argentina
1.027	1.064	1.05	1.07	1.04	1.02	1.075	1.07	1.09	1.04	1.07

words, it is the human behavioural element that we do not model here, but that we glimpse.

Quantifying the effective reproduction numbers accounting for mobility data

We observe that the initial sharp reduction in contact rate due to mobility happened in the middle of March in most regions under study, when initial lockdown was in effect, except in Sweden. The contact rate gradually increased from early May when partial reopening was implemented by governments. The results of these measures are noticeable in the Figs. 4 and 7 upper right panels.

The effect of mobility restrictions throughout 2020 for each geographical location under study is presented in Fig. 5 below. We plot the theoretically estimate $R_{eff-mobile}$ numbers together with the $R_{eff-data}$ effective numbers at each location. Overall, under Google mobility reductions using formula 7, the mobility reduction effect is not enough, on its own, to explain the values

$R_{eff-data}$. This is not surprising, as each location had a varying combination of NPI measures.

Figures 5 (and Fig. 6 in an ensemble view) reveal the reduction in mobility in each region. It seems that the mobility decreased 51% and 54% in Nepal and Italy with respect to the baseline in the first and second weeks of April 2020, respectively. The mobility fell about 20% percent in Indonesia and Sweden. Large-scale social restrictions (sometimes called partial lockdown) were introduced by the Indonesian government in place of nationwide lockdown at the end of March 2020 while the Swedish authorities imposed some restrictions on gatherings in late November.

Human behaviour and its impact on disease transmission
The effects of mask mandates and mask compliance
on further reduction of the effective reproduction numbers

We will be looking at two main tools that populations can use to control the pandemic: *social distancing* and
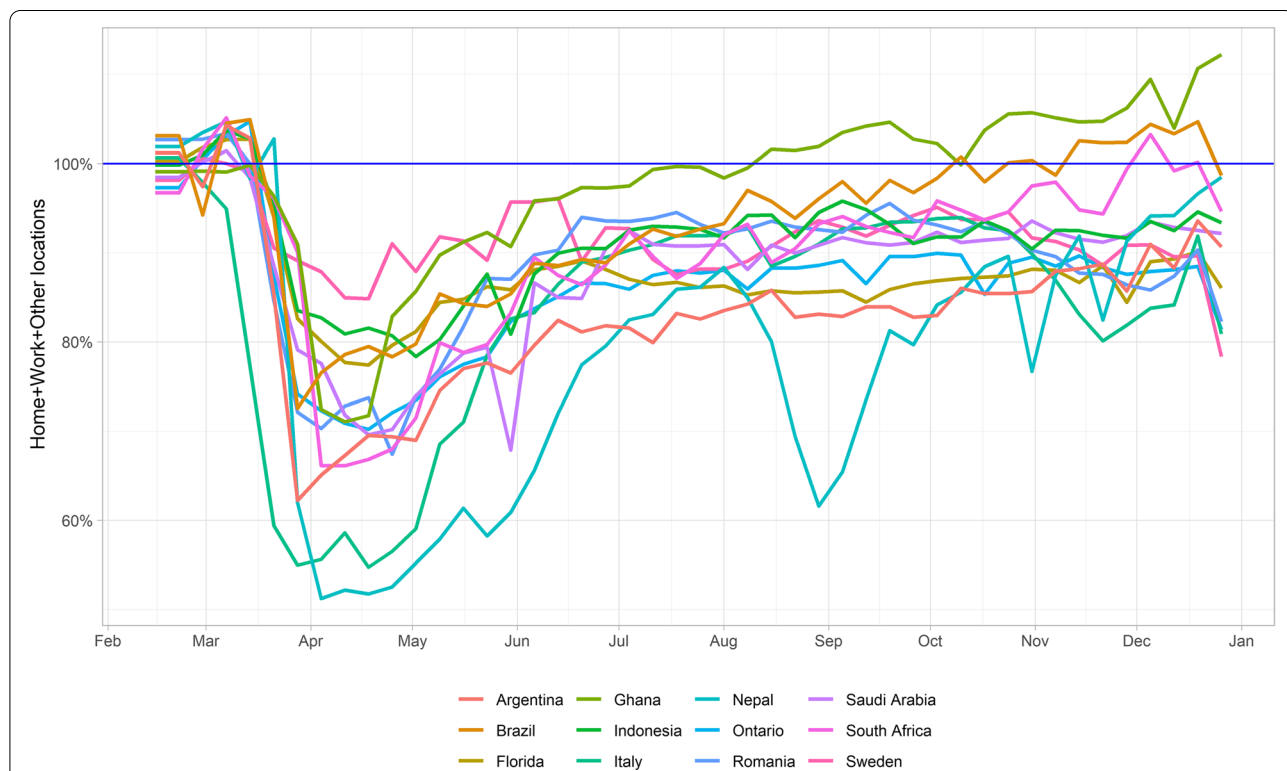
Fig. 4 Average weekly contact rates reflecting mobility changes from the Google Mobility index in the Home, work and other activities respect to the baseline (pre-lockdown), from Feb 15 to Dec 31, 2020. Baseline rates were computed from Google mobility reports over a 6 week interval of January-February 2020

Fig. 5 Effective reproduction numbers from the mobility data influenced by contact rate. In each panel, the red vertical dash line represents the lockdown measures date and the pink curve shows the weekly effective reproduction numbers from the mobility affected by average contact rate in that region
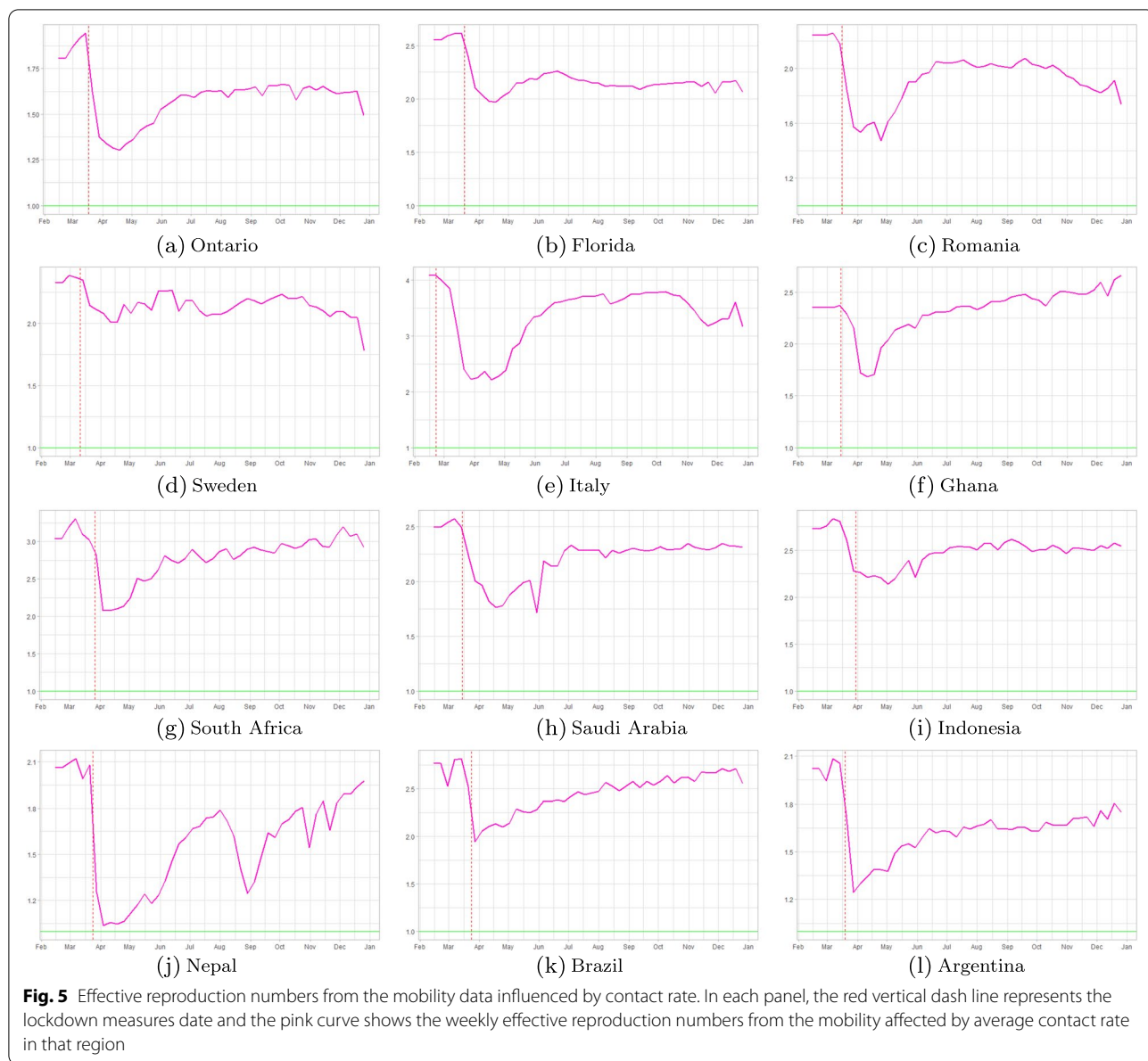
mask wearing. In our framework here, each one of these directly influences the transmission rate β. Denoting by $mask_{eff}$ the efficacy of an average mask at preventing transmission and by $compliance_m$ the compliance with mask wearing let us imagine a meaningful contact between an infected and a susceptible individual: If an individual wears a mask and $mask_{eff}$=0.3, then he/she has an increased protection against transmission. If the individual complies with mask wearing 50% of the time, then their protection due to mask wearing is, on average $mask_{eff} \cdot compliance_m$=0.15 which implies that the

per-contact transmission probability p will decrease with mask wearing:

$$p' = (1 - mask_{eff} \cdot compliance_m) \cdot p$$

Recalling that the level of mask-wearing and social distancing both change over time, we estimate that

$$\beta(t) = contact_{av}(t)(1 - mask_{eff} \cdot compliance_m(t)) \cdot p \tag{8}$$

Let us consider only mask-wearing for the time being. In this paper we use a value of $mask_{eff}$=50%, as averaged based on estimates in [56] (see a more

Mohammadi *et al. BMC Public Health*   (2022) 22:1594

Page 11 of 19

Fig. 6 Reduction in Average weekly contact rates reflecting mobility changes from the Google Mobility index throughout 2020. The week that reduction happened is highlighted by "month/day" in each bar
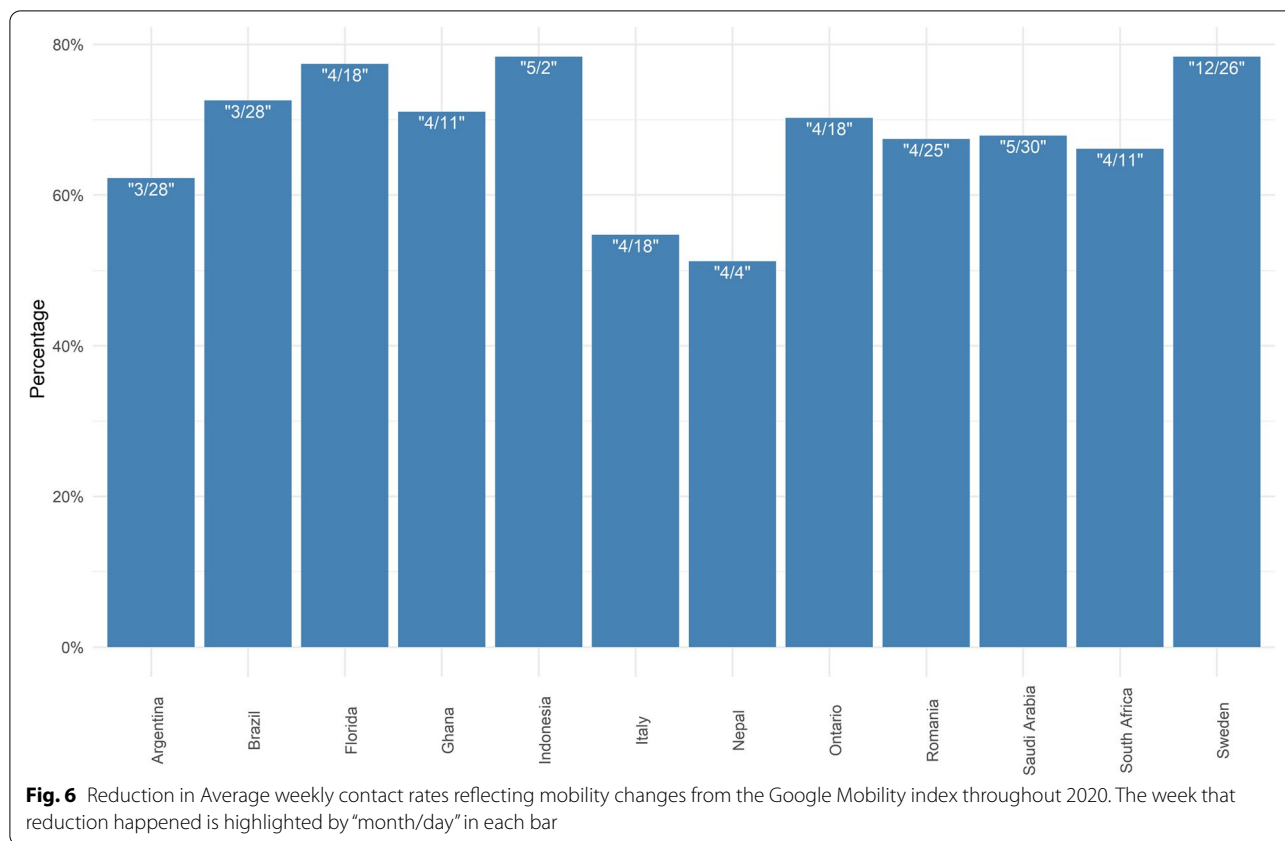
detailed discussion in Additional file 1: Appendix. and the values of mask compliance from IHME (details of data sources in Data sources section above and Additional file 1: Appendix.). Using (8) in the estimate (7) leads to:

$$R_{eff-mobilemask} = \frac{(1 - mask_{eff} \cdot compliance_m(t))contact_{av}(t) \cdot p}{-\epsilon\kappa \cdot a + \epsilon\kappa + \gamma}(1 - \sum_{\tau \in [0,t]} i(\tau)) \qquad (9)$$

with mask compliance data from IHME (see Additional file 1: Appendix) and $contact_{av}(t)$ data that is explained in section (Time-series of effective reproduction numbers accounting for mobility data and projected contact rates).

Figure 7 shows the effective reproduction numbers as obtained from the incidence data (yellow curves) from Fig. 2, together with our theoretical estimates from Fig. 5 (light pink curves) using mobility data, to which now we add a new theoretically estimated $R_{eff-mobilemask}$ number reflecting mask wearing data and formula 9 above. The red and black dashed lines in each panel show the lockdown and mask-wearing mandate dates, respectively, in each region as publicly available.

From 7 we observe that the theoretically-estimated curve using both mobility reductions and mask wearing data (which we will now denote by $R_{eff-mobilemask}$) is accounting for more of the reduction in transmission than the estimated $R_{eff-mobile}$ curves of Fig. 5. Evidently, in some regions (Ontario and Argentina) we observe what it looks like an over-reduction in the values of $R_{eff-mobilemask}$ as compared to $R_{eff-data}$, while in other countries, most notably Sweden, we notice essentially no contribution in further reduction from $R_{eff-mobile}$ to $R_{eff-mobilemask}$. In Sweden's case, this is not surprising, as the mask wearing levels in the IHME data we used hover between 1%−2% throughout 2020. Last but not least, this assumes a values of mask efficacy $mask_{eff}$=50%. If this value is decreased, the $R_{eff-mobilemask}$ curves will shift upwards, i.e. the reduction of $R_{eff-mobile}$ due to mask wearing will be smaller.

Fig. 7 A comparison of the effective reproduction number as obtained from the incidence data (yellow curves), to our theoretical estimate from Section Quantifying the effective reproduction number using incidence data (light pink curves) using mobility data. Beyond the date of mask mandate enactment in each region, we show the theoretically-estimated incidence both with (dark pink) and without (light pink) the added effect of mask-wearing

Effects of other social distancing measures on further reduction of disease spread

As we highlighted in previous section, a host of other NPI's have been employed, at different strengths, across the regions. While it is clear from our investigations thus far that the mobility reduction (as reflected in Google mobility data), along with mask wearing and mask compliance helped tremendously in the de-escalation of the R_{eff} curves, we wish to further analyze the data to extract more information on the strength of other NPI's. Let us

denote by $compliance_{oNPI}$ the compliance level in the local population with *other NPI* measures (by other we mean other than mobility and mask wearing). With this in mind, an average individual in a local population is protected over the course of their contacts proportional to what fraction of the time they also comply with other NPI measures:

$$contact'_{av} = (1 - compliance_{oNPI}(t)) \cdot contact_{av}$$

which then means that

Fig. 8 Effect of other NPI measures (e.g. 6 feet (2m) social distancing, hand washing, etc.) [$R_{eff-data}/R_{eff-mobile}$]. Mandatory masks were introduced at dates represented by the vertical dashed line in each panel
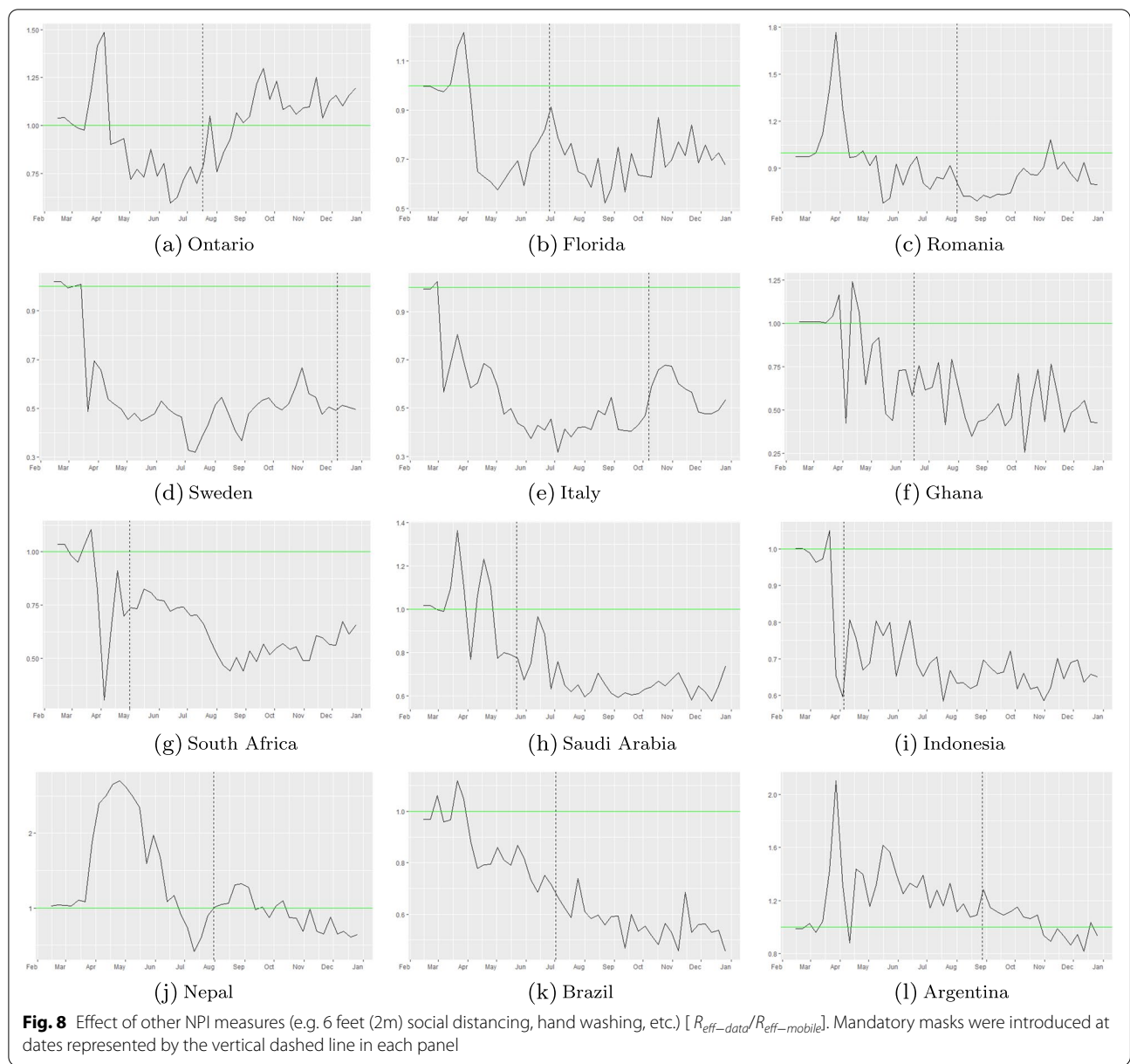
$$R_{eff-data} = (1-compliance_{oNPI}(t))R_{eff-mobilemask} \implies \frac{R_{eff-data}}{R_{eff-mobilemask}} = 1-compliance_{oNPI}(t)$$

This means that to quantify the effects of other NPI measures per region, we further look at the ratio: $\frac{R_{eff-data(t)}}{R_{eff-mobilmask(t)}}$. We present these plots in Fig. 8 below.

Clearly when the ratio is less than 1, then the reduction in the R_{eff} that we quantified from observed data is stronger than the reduction of R_{eff} based on mobility and mask wearing and viceversa. Specifically we obtain the following:

$$\frac{R_{eff-data}}{R_{eff-mobile}} \leq 1 \implies 1 - compliance_{oNPI}(t) \leq 1 \implies compliance_{oNPI}(t) \geq 0$$

Mohammadi *et al. BMC Public Health*   (2022) 22:1594

Page 14 of 19

In the other case, under our assumptions, we get

$$\frac{R_{eff-data}}{R_{eff-mobile}} > 1 \implies compliance_{oNPI} < 0.$$

In cases where $compliance_{oNPI}<0$ we interpret it to mean that perhaps the assumption of 50% efficacy in all regions may have been too optimistic..

One remark is worth to be made at this point: if one decreases the mask efficacy $mask_{eff}$ to an average of 40%, respectively even lower to 30% (as in [56]), then the $R_{eff-mobilemask}$ curves of Fig. 5 would scale equivalently upward by a constant, thus implying that the mask wearing effect is less effective and therefore that the ratio $\frac{R_{eff-data}}{R_{eff-mobile}}$ would be less than 1 (i.e., $compliance_{oNPI}(t)>0$) for most (respectively all) regions.

Results in Sweden in particular stand out (see Fig. 9). They indicate that other NPI measures were extremely effective in reducing the transmission rate of disease, in the absence of mandated lockdown periods and nearly 0 mask wearing. In the case of Sweden for instance (upper panel of Fig. 9), $compliance_{oNPI}(t)$ is large starting in April 2020. Here $compliance_{oNPI}(t)>0$ at and over 50% in Sweden. In case of Indonesia, we estimate that $compliance_{oNPI}(t)$ at and over 30-40% in Indonesia. Both these ranges assume an average of $mask_{eff}=50\%$ over the time period May-December 2020.

At the other end of the spectrum, Ontario (upper left corner panel in Fig. 8) seems to display a ratio of $\frac{R_{eff-data}}{R_{eff-mobile}} \approx 1$ after the mask mandate date (vertical black dash line). Moreover, we have periods of time where the ration is larger than 1 somewhat, so then $compliance_{oNPI}$ might have been negative (in the case where $mask_{eff}=50\%$). This seems to indicate that, under our assumptions, the mobility reductions captured via Google indexes and the mask compliance levels have essentially captured the full picture of the pandemic evolution in this region. Similar trends can be seen in Argentina and Nepal (see Figs. 8 and 10).

Further investigations into mask efficacy and its impact on transmission

In the sections above, we have considered a fixed value of $mask_{eff}=50\%$ across all regions, and we have commented on how a decrease of this value may affect the reductions of $R_{eff-mobile}$ values. From formula 7 we have

$$R_{eff-data} = (1 - mask_{eff} \cdot compliance_m(t))R_{eff-mobile}$$

for each region. Here, we perform a maximum-likelihood estimate of $mask_{eff}$ for each region, such that the fit of $R_{eff-mobile}$ to $R_{eff-data}$ is optimized. In other words, if we considered NPIs to consist only of mask-wearing, what mask efficacy would best reproduce the observed time

series of effective reproduction number in a given region? We present our results in a new plot with a small Table 6:

The graphs of the new $R_{eff-mobilemask}$ time series are presented in Fig. 11 (dark pink curves). Here we see again that Sweden stands out simply because mask wearing was not a policy the population had adopted in 2020; even at a 100% efficacy, an adoption of 1-2% has negligible effect. Thus other NPI factors must have been in play.

Among all the other countries, we see that high levels of mask wearing (for instance in Ontario, and similarly Romania and Argentina) correlates to realistic mask efficacy values (in [56] a realistic expected protection from the mostly cloth-type masks available widely in 2020 is between 30% to 50%) In regions such as Florida, Italy, Indonesia, South Africa, Ghana and Brazil the lower mask wearing levels would have needed to be compensated by higher mask efficacy levels. Since such levels of mask efficacy were not possible in 2020 for an average individual in any of these countries, then other NPI factors had to have been in play.

This analysis furthers the importance of our analysis in the last subsection (Subsection Effects of other social distancing measures on further reduction of disease spread) where we manage to quantify the effect of other NPI factors (*oNPI*) in reductions of transmission in each of the 12 regions.

Conclusion

This paper shows that estimated epidemiological parameters of an underlying SEIR(L) model can be used to compute a time series of effective reproduction numbers accounting for mobility and mask wearing (explicitly using available free data), which are then used to highlight differing pandemic trajectories in very different parts of the world. Our sample consisted of 12 regions (10 countries, 1 Canadian province and 1 US state) chosen based on diversity of population density, median age, urbanization of the population, projected average contact rates, and gross domestic product (GDP) as in Table 1. We used a SEIR(L) epidemiological model (with parameter values from existing literature) and we used it to compute the near disease-free mathematical expressions of the effective reproduction numbers in terms of initial exponential growth of infection. While we made some specific choices on the structure of the compartments and the flow rates between them, we note that the mathematical methodology we applied is universally applicable to other forms of SIR and SEIR models, and not just to ours. This makes our results applicable to many other variants of compartments models for infectious disease transmission, not just for SARS-Cov-2 (for instance the next concern in the wake of the pandemic are the next

Mohammadi *et al. BMC Public Health*   (2022) 22:1594

Page 15 of 19
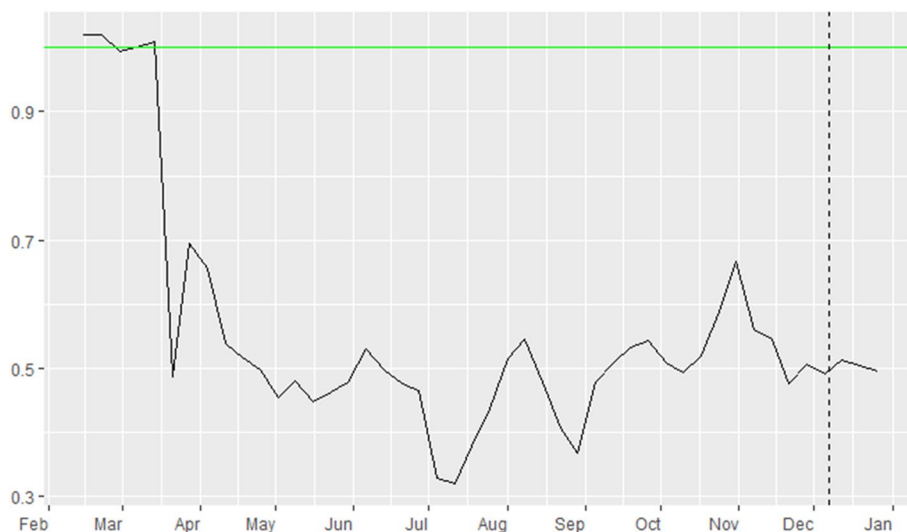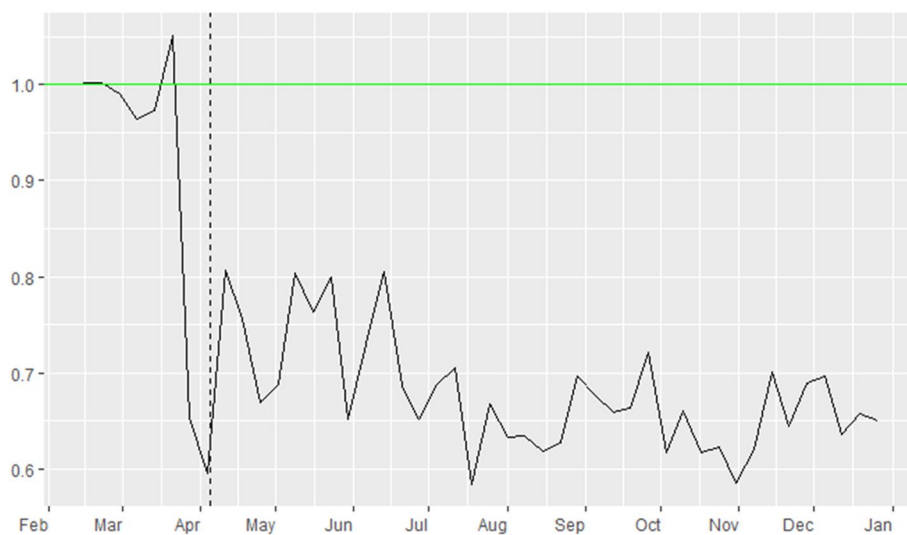
Fig. 9 Effect of other NPI measures in Sweden and Indonesia, [$R_{eff-data}/R_{eff-mobile}$]. Mandatory masks were never introduced in Sweden until November 2020, but they are present earlier in Indonesia. Nationwide lockdown was never used in these countries in 2020

flu seasons and the possible mitigation measures in case high;y infectious flu variants will make an appearance).

We were able to highlight quantitative relationships between the inferred weekly effective reproduction numbers and the estimated weekly effective numbers based on mobility reduction (as captured by Google mobility index) and mask-wearing (as captured from existing data).

Figures 2 and 3 show that there is a sharp drop in $R_{eff-data}$ at the initial lockdown, then most countries have maintained their effective reproduction numbers around

1 by a combination of reduced mobility, mask-wearing and some additional other NPI's. Figure 7 shows a mobility-induced decrease of $R_{eff-mobile}$ with a further decrease when we add mask wearing levels in each region.

Further, our modeling analyses provide direct illustrations of the effectiveness of other NPI's in controlling transmission in each region. Figures 7 and 8 show that effective reproduction numbers in all regions have been helped by population adherence and practice of NPI's over and above reductions in mobility and mask
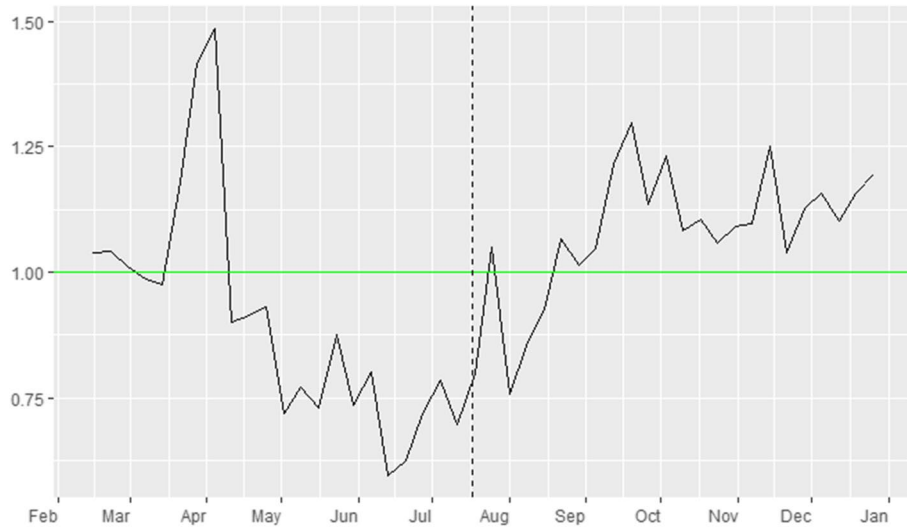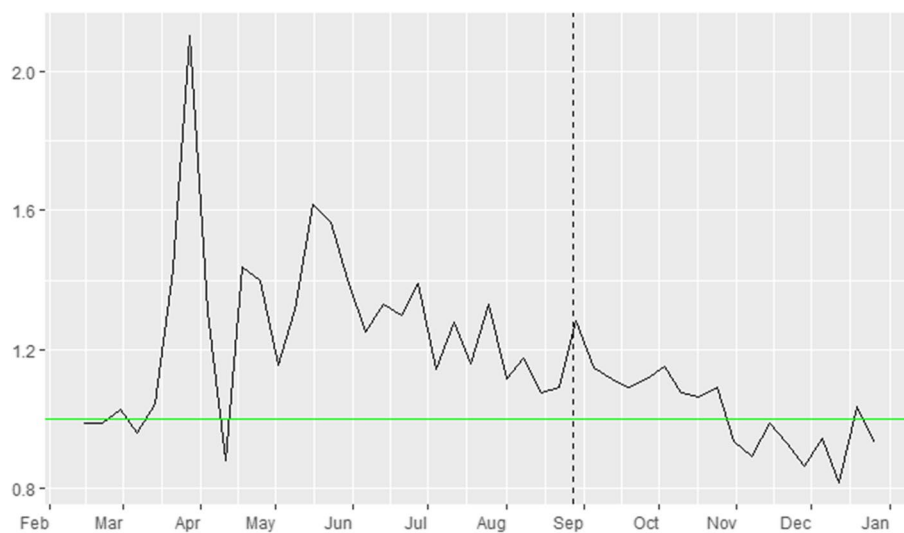
Fig. 10 Effect of other NPI measures in Ontario and Argentina, [$R_{eff-data}/R_{eff-mobile}$]. Mandatory masks were introduced at dates represented by the vertical dashed line in each panel

Table 6 Maximum likelihood best fit values for $mask_{eff}$ per country

Ontario	Florida	Sweden	Italy	Romania	Saudi Arabia	Indonesia	Nepal	South Africa	Ghana	Brazil	Argentina
39%	75%	100%	83%	52%	80%	82%	45%	85%	98%	88%	44%

Fig. 11 Maximum-likelihood estimate of $mask_{eff}$ for each region so that the fit of $R_{eff-mobile}$ to $R_{eff-data}$ is optimized. Curves in dark pink color are the new $R_{eff-mobilemask}$ estimates, where for each country we use the deduced value of $mask_{eff}$ listed
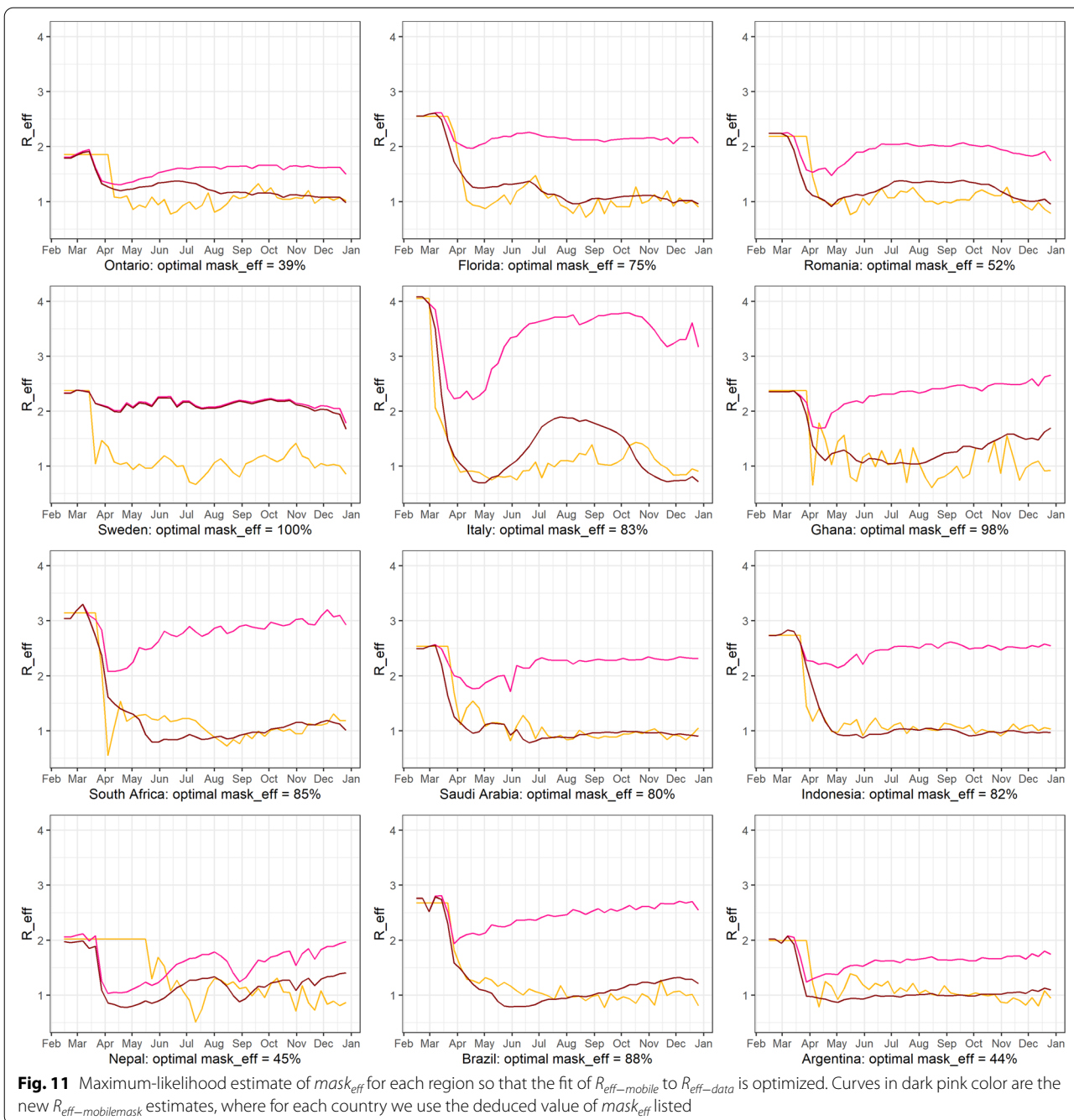
protection. This is also obvious by comparing the values of the effective reproductions numbers inferred from data versus (in Fig. 7 most regions maintain their values in the neighborhood of 1), while mobility reduction alone (as illustrated from Google mobility reports and in Fig. 4) has steadily decrease beyond May 2020 in all locations.

There are several assumptions underlying our study. Clearly, the mobility reduction as reflected in Google mobility reports is used here as representative across each of the populations, however that may not be quite accurate and it depends on the percentage of cellphone usage in a region and whether or not that percentage can be considered representative of an average individual. At the same time, the pre-pandemic projected contact rates from [21] are themselves estimates, thus subject to further change or calibration, given the wealth of data from last year studies.

Nevertheless, the overall ideas we followed are fairly straightforward and the quantification of the control on

Mohammadi *et al. BMC Public Health*   (2022) 22:1594

Page 18 of 19

the pandemic via time series of effective reproduction numbers can be done as shown by using parameter values and data, without the need to model and fit SEIR model curves. Even if some of the assumptions/values in our analysis change, the methodology we propose is flexible, novel and easy to follow and implementing any new or updated piece of data available is straightforward. As future directions of research we are interested in using differing data sources for contact rates in some regions and differing estimates for mobility reductions to replace the Google mobility reports. We can also use differing $S(E)IR$ models and more data on socio-economic and demographic factors that may lead to further insights into accounting for differences in pandemic evolution in diverse countries around the world.

Supplementary Information

The online version contains supplementary material available at (https://doi.org/10.1186/s12889-022-13921-3).

Additional file 1. Appendix

Declarations

Ethics approval and consent to participate
This study does not require ethical approval. All data used or analyzed in this study are freely available in the public domain, and all methods are obtained directly from cited researchers. There is no direct interaction between the researchers and any individual or group in this study.

Consent for publication
Not applicable.

Competing interests
The authors declare that they have no competing interests.

Author details
[1]Department of Mathematics & Statistics, University of Guelph, 50 Stone Road E., Guelph N1G 2W1, Canada. [2]Modeling, Epidemiology and Data Science, Sanofi Pasteur, Toronto, Canada.

References

1. Li Q, Guan X, Wu P, Wang X, Feng Z. Early transmission dynamics in wuhan, china, of novel coronavirus-infected pneumonia. 2020. https://doi.org/10.1056/NEJMoa2001316.
2. Liu Y, Gayle AA, Wilder-Smith A, Rocklöv J. The reproductive number of covid-19 is higher compared to SARS coronavirus. 2020. https://doi.org/10.1093/jtm/taaa021.
3. Cauchemez S, Boëlle P-Y, Thomas G, Valleron A-J. Estimating in real time the efficacy of measures to control emerging communicable diseases. Am J Epidemiol. 2006; 164(6):591–97. https://doi.org/10.1093/aje/kwj274.
4. Stutt ROJH, Retkute R, Bradley M, Gilligan CA, Colvin J. A modelling framework to assess the likely effectiveness of facemasks in combination with 'lock-down' in managing the covid-19 pandemic. 2021; 476(2238). https://doi.org/10.1098/rspa.2020.0376.
5. Eikenberry SE, Mancuso M, Iboi E, Phan T, Eikenberry K, Kuang Y, Kostelich E, Gumel AB. To mask or not to mask: Modeling the potential for face mask use by the general public to curtail the covid-19 pandemic. 2020; 5:293–308. https://doi.org/10.1016/j.idm.2020.04.001.
6. Lau JTF, Tsui H, Lau M, Yang X. Sars transmission, risk factors, and prevention in Hong Kong. 2004; 10(4):587–92.
7. Wu J, Xu F, Zhou W, Feikin DR, Lin C-Y, He X, Zhu Z, Liang W, Chin[†] DP, Schuchat A. Risk factors for SARS among persons without known contact with SARS patients, Beijing, China. 2004; 10(2):210–16.
8. Giordano G, Blanchini F, Bruno R, Colaneri P, Filippo AD, Matteo AD, Colaneri M. Modelling the covid-19 epidemic and implementation of population-wide interventions in Italy. 2020; 26:855–60. https://doi.org/10.1038/s41591-020-0883-7.
9. Kucharski AJ, Russell TW, Diamond C, Liu Y, Edmunds J, Funk S, et al. Early dynamics of transmission and control of covid-19: a mathematical modelling study. 2020; 20(5):553–58. https://doi.org/10.1016/S1473-3099(20)30144-4.
10. Zoltan Neufeld HK, Czirok A. Targeted adaptive isolation strategy for covid-19 pandemic. 2020; 5:357–61. https://doi.org/10.1016/j.idm.2020.04.003.
11. Dandekar R, Henderson SG, Jansen M, Moka S, Nazarathy Y, Rackauckas C, Taylor PG, Vuorinen A. Safe blues: A method for estimation and control in the fight against covid-19. 2020. https://doi.org/10.1101/2020.05.04.20090258.
12. Khataee H, Scheuring I, Czirok A, Neufeld Z. Effects of social distancing on the spreading of covid-19 inferred from mobile phone data. 2021; 11(1661). https://doi.org/10.1038/s41598-021-81308-2.
13. Kain MP, Childs ML, Becker AD, Mordecai EA. Chopping the tail: how preventing superspreading can help to maintain covid-19 control. 2021; 34. https://doi.org/10.1016/j.epidem.2020.100430.
14. de Oliveira SB, Pôrto VBG, Ganem F, Mendes FM, Almiron M, de Oliveira WK, Fantinato FFST, de Almeida WAF, de Macedo Borges Junior AP, Pinheiro HNB, dos Santos Oliveira R, Andrews JR, Faria NR, Lopes MB, de Araújo WN, DiazQuijano FA, Nakaya HI, Croda J. Monitoring social distancing and SARS-cov-2 transmission in brazil using cell phone mobility data. 2020. https://doi.org/10.1101/2020.04.30.20082172.
15. Basellini U, Alburez-Gutierrez D, Fava ED, Perrotta D, Bonetti M, Camarda CG, Zagheni E. Linking excess mortality to mobility data during the first wave of covid-19 in england and wales. SSM - Popul Health. 2021; 14:100799. https://doi.org/10.1016/j.ssmph.2021.100799.
16. Kartal MT, Depren Özer, Depren SK. The relationship between mobility and covid-19 pandemic: Daily evidence from an emerging country by causality analysis. Transp Res Interdisc Perspect. 2021; 10:100366. https://doi.org/10.1016/j.trip.2021.100366.

Mohammadi *et al. BMC Public Health* (2022) 22:1594

Page 19 of 19

17 Ilin C, Annan-Phan S, Xiao HuiTai SM, Hsiang S, Blumenstock JE. Public mobility data enables covid-19 forecasting and management at local and global scales. Sci Rep. 2021; 11(13531). https://doi.org/10.1038/s41598-021-92892-8.

18 Sadowski A, Galar Z, Walasek R, Zimon G, Engelseth P. Big data insight on global mobility during the covid-19 pandemic lockdown. J Big Data. 2021; 8(78). https://doi.org/10.1186/s40537-021-00474-2.

19 Cot C, Cacciapaglia G, Sannino F. Mining google and apple mobility data: temporal anatomy for covid-19 social distancing. Sci Rep. 2021; 11(4150). https://doi.org/10.1038/s41598-021-83441-4.

20 Fields R, Humphrey L, Flynn-Primrose D, Mohammadi Z, Nahirniak M, Thommes E, Cojocaru M. Age-stratified transmission model of covid-19 in ontario with human mobility during pandemic's first wave. Heliyon. 2021; 7(9):07905.

21 Prem K, Cook AR, Jit M. Projecting social contact matrices in 152 countries using contact surveys and demographic data. PLoS Comput Biol. 2017; 13(9):1005697.

22 Mistry D, Litvinova M, y Piontti AP, Chinazzi M, Fumanelli L, Gomes MFC, Haque SA, Liu Q-H, Mu K, Xiong X, Halloran ME, Jr. IML, Merler S, Ajelliy M, Vespignani A. Inferring high-resolution human mixing patterns for disease modeling. 2021; 323(12). https://doi.org/10.1038/s41467-020-20544-y.

23 Mossong J, Hens N, Jit M, Beutels P, Auranen K, Mikolajczyk R, Massari M, Salmaso S, Tomba GS, Wallinga J, et al. Social contacts and mixing patterns relevant to the spread of infectious diseases. PLoS Med. 2008; 5(3):74.

24 Feehan DM, Mahmud AS. Quantifying population contact patterns in the united states during the covid-19 pandemic. 2021; 12(893). https://doi.org/10.1038/s41467-021-20990-2.

25 Zhang J, Litvinova M, Liang Y, Wang Y, Wang W, Zhao S, Wu Q, Merler S, Viboud C, Vespignani A, Ajelli M, Yu1 H. Changes in contact patterns shape the dynamics of the covid-19 outbreak in china. 2020; 368(6498):1481–86. https://doi.org/10.1126/science.abb8001.

26 Jarvis CI, Zandvoort KV, Gimma A, Prem K, Klepac P, Rubin GJ, and WJE. Quantifying the impact of physical distance measures on the transmission of COVID-19 in the UK. 2020. https://doi.org/10.1101/2020.03.31.20049023.

27 Latsuzbaia A, Herold M, Bertemes J-P, Mossong J. Evolving social contact patterns during the covid-19 crisis in luxembourg. 2020; 15:e0237128. https://doi.org/10.1371/journal.pone.0237128.

28 Fava ED, Cimentada J, Perrotta D, André Grow FR, Gil-Clavel S, Zagheni E. The differential impact of physical distancing strategies on social contacts relevant for the spread of covid-19. 2020. https://doi.org/10.1101/2020.05.15.20102657.

29 Prem K, Liu Y, Kucharski TWRAJ, Eggo RM, Davies N, for the Mathematical Modelling of Infectious Diseases COVID-19 Working Group C, Jit M, Klepac P. The effect of control strategies to reduce social mixing on outcomes of the covid-19 epidemic in wuhan, china: a modelling study. 2020; 5(5):261–70. https://doi.org/10.1016/S2468-2667(20)30073-6.

30 Prem K, van Zandvoort K, Klepac P, Eggo1 RM, Davies NG, for the Mathematical Modelling of Infectious Diseases COVID-19 Working Group C, Cook AR, Jit M. Projecting contact matrices in 177 geographical regions: an update and comparison with empirical data for the covid-19 era. 2020. https://doi.org/10.1101/2020.07.22.20159772.

31 Spouge JL. A comprehensive estimation of country-level basic reproduction numbers r0 for covid-19: Regime regression can automatically estimate the end of the exponential phase in epidemic data. 2021; 16(7). https://doi.org/10.1371/journal.pone.0254145.

32 Liua Y, Gua Z, Xiab S, Shib B, Zhoub X-N, Shig Y, Liu J. What are the underlying transmission patterns of covid-19 outbreak? an age-specific social contact characterization. 2020; 22. https://doi.org/10.1016/j.eclinm.2020.100354.

33 Brankston G, Merkley E, Fisman DN, Tuite AR, Poljak Z, Loewen PJ, Greer AL. Quantifying contact patterns in response to covid-19 public health measures in canada running title: Contact patterns during covid-19 in canada. 2021. https://doi.org/10.1101/2021.03.11.21253301.

34 van den Driessche P. Reproduction numbers of infectious disease models. Infect Dis Model. 2017; 2(3):288–303.

35 COVID-19 Data Repository by the Center for Systems Science and Engineering (CSSE) at Johns Hopkins University. https://github.com/CSSEGISandData/COVID-19. Accessed Aug 2022.

36 Tuite AR, Fisman DN, Greer AL. Mathematical modelling of covid-19 transmission and mitigation strategies in the population of ontario, canada. CMAJ. 2020; 192(19):497–505.

37 Mizumoto K, Kagaya K, Zarebski A, Chowell G. Estimating the asymptomatic proportion of coronavirus disease 2019 (COVID-19) cases on board the diamond princess cruise ship, yokohama, japan, 2020. Eurosurveillance. 2020; 25(10). https://doi.org/10.2807/1560-7917.es.2020.25.10.2000180.

38 He W, Yi GY, Zhu Y. Estimation of the basic reproduction number, average incubation time, asymptomatic infection rate, and case fatality rate for COVID-19: Meta-analysis and sensitivity analysis. J Med Virol. 2020. https://doi.org/10.1002/jmv.26041.

39 Ontario PH. COVID-19 – What We Know So Far About... Asymptomatic Infection and Asymptomatic Transmission. https://www.publichealthontario.ca/-/media/documents/ncov/what-we-know-jan-30-2020.pdf?la=en. Accessed 19 June 2020.

40 Wu J, Tang B, Bragazzi NL, Nah K, McCarthy Z. Quantifying the role of social distancing, personal protection and case detection in mitigating COVID-19 outbreak in ontario, canada. J Math Ind. 2020; 10(1). https://doi.org/10.1186/s13362-020-00083-3.

41 Asgary A, Cojocaru MG, Najafabadi MM, Wu J. Simulating preventative testing of SARS-cov-2 in schools: policy implications. BMC Public Health. 2021; 21(1):1–18.

42 Humphrey L, Thommes EW, Fields R, Hakim N, Chit A, Cojocaru MG. A path out of covid-19 quarantine: an analysis of policy scenarios. medRxiv. 2020. https://doi.org/10.1101/2020.04.23.20077503. https://www.medrxiv.org/content/early/2020/04/29/2020.04.23.20077503.full.pdf.

43 Van den Driessche P. Reproduction numbers of infectious disease models. Infect Dis Model. 2017; 2(3):288–303.

44 Pellis L, Birrell PJ, Blake J, Overton CE, Scarabel F, Stage HB, Brooks-Pollock E. Estimation of reproduction numbers in real time: concep-tual and statistical challenges. Journal of the Royal Statistical Society: Series A. 2021.

45 COVID-19 Pandemic in Sweden. 2020; https://en.wikipedia.org/wiki/COVID-19_pandemic_in_Sweden#cite_ref-170. Accessed Aug 2022.

46 Jenelius E, Cebecauer M. Impacts of covid-19 on public transport ridership in sweden: Analysis of ticket validations, sales and passenger counts. Transp Res Interdiscip Perspect. 2020; 8:100242.

47 Hovne A. Nära Var Tredje Bil Borta Från Stockholms Gator. Omni (in Swedish). https://omni.se/nara-var-tredje-bil-borta-fran-stockholms-gator/a/awQ7jL. Accessed 31 Mar 2020.

48 Henley. Critics Question Swedish Approach as Coronavirus Death Toll Reaches 1,000. The Guardian. https://www.theguardian.com/world/2020/apr/15/sweden-coronavirus-death-toll-reaches-1000. Accessed 15 Apr 2020.

49 Google. COVID-19 Community Mobility Reports. 2020. https://www.google.com/covid19/mobility/. Accessed 15 Feb 2020.

50 Statistics Canada: Population estimates. https://www150.statcan.gc.ca/t1/tbl1/en/tv.action?pid=1710000501&pickMembers%5B0%5D=1.1&pickMembers%5B1%5D=2.1&cubeTimeFrame.startYear=2016&cubeTimeFrame.endYear=2020&referencePeriods=20160101%2C20200101. Accessed Jul 2020.

51 United States Census. https://data.census.gov/cedsci/table?q=Florida&tid=ACSST1Y2019.S0101&hidePreview=false. Accessed 2019.

52 United Nations. World age distribution. 2019. https://population.un.org/wpp/Download/Standard/Population/. Accessed 2019.

53 The Institute for Health Metrics and Evaluation, Compliance with Mask. https://covid19.healthdata.org/. Accessed 4 June 2021.

54 London YIC. How Often Have You Worn a Face Mask Outside Your Home to Protect Yourself or Others from Coronavirus (COVID-19)?https://www.statista.com/statistics/1114375/wearing-a-face-mask-outside-in-european-countries/. Accessed 10 Jan 2021.

55 Fields R, Humphrey L, Thommes EW, Cojocaru MG. COVID-19 in Ontario: Modelling the Pandemic by Age Groups Incorporating Preventative Rapid-Testing. In: Murty VK, Wu J. (eds) Mathematics of Public Health. Fields Institute Communications, vol 85. Cham: Springer; 2022. https://doi.org/10.1007/978-3-030-85053-1_4.

56 Wilson AM, Abney SE, King M-F, Weir MH, López-García M, Sexton JD, Dancer SJ, Proctor J, Noakes CJ, Reynolds KA. Covid-19 and use of non-traditional masks: how do various materials compare in reducing the risk of infection for mask wearers?J Hosp Infect. 2020; 105(4):640–42.

Publisher's Note